Curvature-Induced Configuration Transition in Confined Nematic Liquid Crystals

R. J. Ondris-Crawford, G. P. Crawford, S. Žumer,[a] and J. W. Doane
Liquid Crystal Institute and Department of Physics, Kent State University, Kent, Ohio 44242-0001
(Received 11 September 1992)

Stable nematic director fields of liquid crystals confined to cylindrical cavities which enforce homogeneous concentric anchoring depend on the competition between azimuthal and polar molecular anchoring strengths and the surface elastic constant K_{24}. Deuterium nuclear-magnetic-resonance line shapes of such systems reveal a structural transition from an escaped-twisted to a newly discovered planar-bipolar configuration as the curvature is varied. This observation allows for the first determination of the polar and azimuthal anchoring energies and K_{24} by a single experimental method.

PACS numbers: 64.70.Md, 61.30.Cz, 61.30.Jf, 68.10.Cr

One of the most important physical parameters that characterizes the solid–liquid-crystal interface is the orientational molecular anchoring strength [1]. The free energy associated with this interaction can be expressed phenomenologically as the vector sum of the azimuthal (in-plane) and polar (out-of-plane) component [2]. Several techniques have been developed to measure both components for a variety of liquid crystals and substrates [3] with homogeneous [4] and homeotropic anchoring [5].

It has proved to be a difficult task to simultaneously measure both the azimuthal and polar anchoring strengths [6]. These parameters become even more elusive when liquid crystals are confined to submicrometer environments, e.g., spheres [7] and cylinders [8]. The presence of bulk and surface elastic deformations along with the effect of finite anchoring energies complicates both the theoretical and experimental analysis in these systems. Recently, it was reported that the effects of polar anchoring energies could be separated from the surface nematic elastic energies by probing the nematic director fields that occur in the submicrometer cylindrical cavities using deuterium nuclear magnetic resonance (^{2}H-NMR) [8,9].

Little is known about the nature of the interactions occurring at the surface when parallel anchoring conditions are enforced in confined geometries. Cladis and Kleman first predicted that in a nematic phase confined to a cylindrical cavity an escaped-twisted (ET) structure (see Fig. 1) is stable under strong concentric parallel anchoring conditions, where the molecules are parallel to the cylinder surface yet perpendicular to its symmetry axis [10]. They calculated this structure to transform into a planar-concentric (PC) structure when the elastic free energy becomes favorable (see Fig. 1) [10]. Only one attempt to obtain these structures experimentally has been reported [11], but nonuniform concentric rubbing of the inner cavity wall resulted in irregularities of the director field.

In this contribution we provide the first experimental study of nematic director fields in cylindrical regions when concentric parallel anchoring conditions are enforced. Analysis of the Frank free energy supplemented by the appropriate anchoring energy terms reveals structures sensitive to the polar and azimuthal anchoring strengths and the surface elastic constant K_{24}.

We overcome the experimental hurdles in obtaining these unusual configurations by modifying the inner walls of the cylindrical cavities of polycarbonate Nuclepore (Nuclepore Corp.) membranes [see Fig. 2(a)] with a

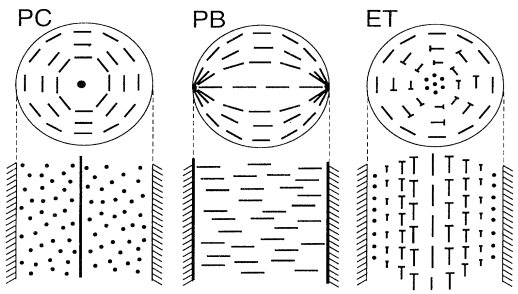

FIG. 1. Possible nematic director field structures in cylindrical environments when parallel anchoring is preferred: the planar-concentric (PC), planar-bipolar (PB), and escaped-twisted (ET) structure, where the top of the nails represents that part of the director beneath the plane of the cross section.

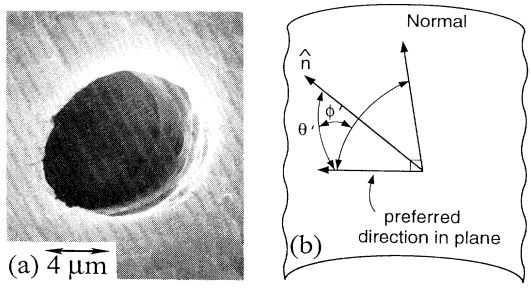

FIG. 2. The inner corrugated walls of a cylindrical cavity of Nuclepore membranes as revealed by scanning electron microscopy (SEM) (a). A representation of the angles used in the calculation of the director fields on the surface of the cavities (b).

Polyimide (Du Pont) treatment. The large number (pore density $\sim 3\times 10^8/\mathrm{m}^2$) of these circumferentially corrugated cavities [12] are filled with the liquid-crystal compound 4'-pentyl-4-cyanobiphenyl (5CB-βd_2). The anchoring and surface elastic properties are expected to be important in cavities with submicron size diameters. A variety of sizes ranging from 0.1 to 0.5 μm in radius is employed that is much smaller than the resolution of an optical microscope. Therefore NMR is used to study the nematic director fields within these pores. We should point out that the pore sizes mentioned in this Letter are nominal pore sizes provided by the manufacturer. For example the measured [13] radius for a nominal pore radius of 0.1 μm is 0.0825($\pm$0.0075) μm. The pore size distribution, however, is very narrow with 80% of the pores being within 10% of the mean of 0.085 μm.

The total free energy of a confined liquid crystal is expressed as

$$F=\tfrac{1}{2}\int_{\mathrm{vol}}\{K_{11}(\nabla\cdot\mathbf{n})^2+K_{22}(\mathbf{n}\cdot\nabla\times\mathbf{n})^2+K_{33}(\mathbf{n}\times\nabla\times\mathbf{n})^2-K_{24}\nabla\cdot(\mathbf{n}\times\nabla\times\mathbf{n}+\mathbf{n}\nabla\cdot\mathbf{n})\}dV$$
$$+\tfrac{1}{2}\int_{\mathrm{surf}}(W_\phi\sin\phi'+W_\theta\cos\phi')\sin^2\theta'\,dS\,, \qquad (1)$$

where K_{11}, K_{22}, and K_{33} are the conventional splay, twist, and bend bulk elastic constants, respectively, and $\mathbf{n}$ is the nematic director. The saddle-splay surface elastic constant K_{24} is a material parameter that is independent of interactions occurring at the substrate. The final two terms which represent the interfacial free energy are described by the azimuthal W_ϕ and polar W_θ anchoring strengths and θ' and ϕ' are explained in Fig. 2(b).

The PC configuration (see Fig. 1), a planar director field with a pure bend deformation and line disclination along the symmetry axis of the cylinder, is a possible solution to Eq. (1) for the above anchoring conditions [10]. The free energy per unit length, $F_{\mathrm{PC}}=\pi K_{33}\ln(R/\rho_{\mathrm{PC}})$, where ρ_{PC} is the radius of the core of the line disclination [14], is independent of K_{24} and W_ϕ (or W_θ).

We have discovered that under these conditions the PC configuration does not yield the lowest free energy. A planar-bipolar (PB) structure (see Fig. 1) has a planar director field with a splay-bend deformation and two surface disclination lines running parallel to the symmetry axis of the cylinder connecting the poles of the planar field. It is completely specified by $\mathbf{n}=\cos\Psi(r,\phi)\mathbf{i}_r+\sin\Psi(r,\phi)\mathbf{i}_\phi$, where Ψ is the angle between the radial vector $\mathbf{r}$ and the local nematic director, and ϕ is the angle between the radial vector and the symmetry axis of the structure. For infinitely strong anchoring at the cavity wall the free energy per unit length in the one-constant approximation ($K_{11}=K_{33}=K$) is given by $F_{\mathrm{PB}}=\pi K\times\ln(R/4\rho_{\mathrm{PB}})$, where ρ_{PB} is the radius of the cores of the two disclination lines. For the above-mentioned approximation, leading to $\rho_{\mathrm{PB}}=\rho_{\mathrm{PC}}$, the free energy of the PB structure is always lower than that of the PC structure. Introducing finite anchoring the nematic director distribution can be obtained in closed form by solving the Euler-Lagrange equation by a conformal mapping technique to yield

$$\Psi=\tan^{-1}\{\cot\phi(R^2+\gamma r^2)/(R^2-\gamma r^2)\}\,, \qquad (2)$$

where $\gamma=(\xi^2+1)^{1/2}-\xi$ and $\xi=2K/RW_\theta$. The finite anchoring condition eliminates the presence of both surface disclination lines of the structure. The free energy per unit length is $F_{\mathrm{PB}}=\pi K\{-\ln(2\gamma\xi)+(1-\gamma)/\xi\}$.

The ET configuration is also a defectless director field (see Fig. 1). Its bend-twist deformation is specified in cylindrical coordinates by $\mathbf{n}=\sin\alpha(\mathbf{r})\mathbf{i}_\phi+\cos\alpha(\mathbf{r})\mathbf{i}_z$, where α is the angle between the local nematic director and the cylinder axis [10]. We present a generalization of this structure by including the K_{24} term and allowing for the smooth change of the surface nematic director from a concentric to an axial direction by varying the anchoring strength. The minimization of Eq. (1) results in the equilibrium configuration given by

$$\frac{r}{R}=\left[\frac{[1+(\kappa-1)\sin^2\alpha]^{1/2}-\cos\alpha}{[1+(\kappa-1)\sin^2\alpha]^{1/2}+\cos\alpha}\left(\frac{\sigma+1}{\sigma-1}\right)\right]^{1/2}, \qquad (3)$$
$$\kappa\equiv\frac{K_{33}}{K_{22}}>1\,,$$

where $\sigma\equiv RW_\phi/K_{22}+K_{24}/K_{22}-1$ is a dimensionless surface parameter describing the effective anchoring strength at the surface. The free energy per unit length in the one-constant approximation is $F_{\mathrm{ET}}=\pi K(3-K_{24}/K-1/\sigma)$.

Equating the free energies for the PB and ET structure in the finite anchoring regime at a critical radius R_c, a three-dimensional stability diagram in terms of the dimensionless surface parameters RW_θ/K, RW_ϕ/K, and K_{24}/K is created (see Fig. 3). The phase diagram is calculated for the one-constant approximation. A more detailed analysis for nonequal elastic constants is desirable and will be published at a later time.

The ^{2}H-NMR spectral pattern directly reflects the director distribution of the sample via the quadrupole frequencies expressed as $\delta\nu_q=\pm\frac{1}{2}\delta\nu_B[3\cos^2\Theta(\mathbf{r})-1]$ where $\Theta(\mathbf{r})$ is the angle between the local nematic director $\mathbf{n}$ and the applied magnetic field, and $\delta\nu_B$ is the quadrupole splitting of the aligned bulk in the nematic phase [15]. The NMR magnetic field has a negligible effect on the configuration inside the cavity since the magnetic coherence length, $\xi_m=(\mu_0K_{22}/\Delta\chi)^{1/2}/B\sim 1.2$ μm, is larger than the cavity diameter, using reported values for the anisotropy in the diamagnetic susceptibility, $\Delta\chi=2.8\times10^{-7}$, the twist elastic constant $K_{22}=4\times10^{-12}$

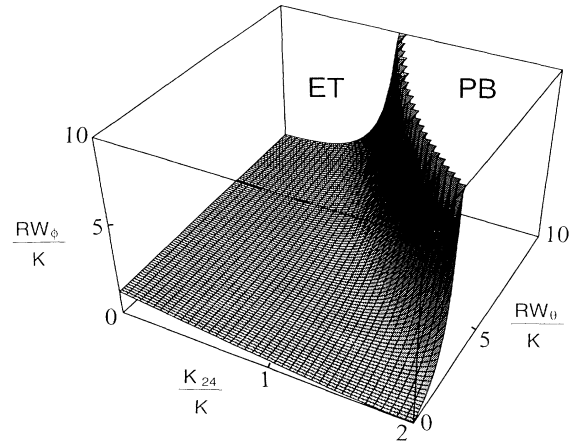

FIG. 3. A stability diagram for the escaped-twisted and planar-bipolar structures in terms of dimensionless surface parameters.

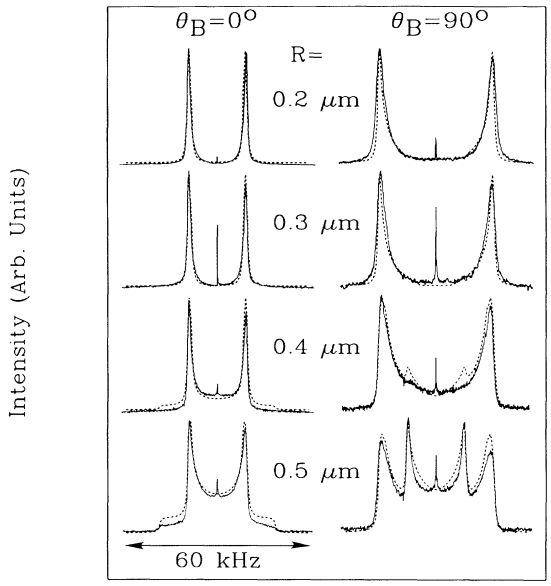

FIG. 4. ^{2}H-NMR line shapes of 5CB-βd_2 confined in Polyimide-modified Nuclepore membranes recorded at room temperature. The dashed lines correspond to the theoretical fits. The $R=0.4$ μm theoretical spectra are composed of 15% ET and 85% PB and the $R=0.5$ μm spectra of 50% ET and 50% PB. We attribute the narrow central peak to an artifact produced by our NMR machine.

J/m, and the strength of our magnetic field $B=4.7$ T. The extent of the effect of diffusion on the NMR line shape is also negligible since the distance the molecule migrates on the NMR time scale, $x_0 \sim (D/\delta\nu)^{1/2} \sim 0.02$ μm, is substantially smaller than the cavity diameter for typical values of the self-diffusion constant $D \sim 10^{-11}$ m^2/s and the bulk value of $\delta\nu_B = 40$ kHz. The experimental ^{2}H-NMR line shapes are directly compared to simulations using the calculated structures. This is performed for the cylinders parallel ($\theta_B = 0°$) and perpendicular ($\theta_B = 90°$) to the magnetic field (see Fig. 4) to differentiate between the structures.

For cavity sizes $R=0.2$ and 0.3 μm, the spectral patterns reveal the existence of the PB configuration observed for the first time. The $\theta_B = 0°$ line shape confirms the planar nature of the structure while the $\theta_B = 90°$ line shape clearly discriminates between the PC and PB structure, since a PC structure would reveal a cylindrical powder pattern (four peaks) at this orientation. The PB structure gives rise to the observed two peaks separated by the bulk splitting $\delta\nu_B$. The NMR magnetic field, as mentioned above, is not strong enough to substantially distort the director field itself. However, the two peaks in the $\theta_B = 90°$ spectrum indicate that this relatively weak field does reorient the symmetry axes of the PB structure to within a few degrees of the $\theta_B = 90°$ orientation due to the spherical cross section of the cavities. These conclusions are supported by a qualitative polarizing optical microscope observation of the transmitted light along the large collection of small cylindrical cavities. The modulation of transmitted light caused by a gradual application of a transverse electric field clearly indicates the gradual reorientation of the symmetry axis of the PB structure parallel to the applied field. Only the NMR spectra are sensitive enough to study the dependence of the PB structure on the dimensionless parameter RW_θ/K, which can be directly determined by fitting the theoretical [using Eq. (2)] to the experimental $\theta_B = 90°$ PB line shapes (see Fig. 4). By fitting the $\theta_B = 90°$ line shapes for both PB samples, the value of W_θ is found to be $(1 \pm 0.4) \times 10^{-4}$ J/m^2 using an average value of $K = 7.0 \times 10^{-12}$ J/m.

Increasing the pore size from $R=0.3$ μm to $R=0.5$ μm the line shapes experience a dramatic change revealing the transition to the ET structure, which starts to appear in a small percentage of pores in the $R=0.4$ μm sample. Because of the distribution of cylinder sizes inherent in Nuclepore membranes [13] some cylinders still support the PB structure even at $R=0.5$ μm. Both $\theta_B = 0°$ and 90° orientations are sensitive to the parameter $\sigma = RW_\phi/K_{22} + K_{24}/K_{22} - 1$. Two fitting parameters are therefore required to calculate the theoretical spectra: the ratio of PB to ET and the value of σ. Fitting the spectra concludes that the $R=0.4$ μm sample consists of 15% ET and 85% PB structures and the $R=0.5$ μm sample of 50% ET and 50% PB structures; the value of σ is found to be 12 ± 1. By taking into account point defects along the symmetry axis of the cylinder due to oppositely escaping domains [15], the shoulders in the theoretical fits for the $\theta_B = 0°$ orientations as well as the inner peaks in the $\theta_B = 90°$ orientation can be reduced, resulting in better fits to the experimental spectra. The latter is beyond the scope of this Letter and is the subject of a

future more precise study. Using $K_{24}/K_{22} \sim 2$ [8] and $K_{22} = 4 \times 10^{-12}$ J/m, W_ϕ is determined to be $(0.8 \pm 0.4) \times 10^{-4}$ J/m^2.

The magnitude of W_θ and W_ϕ are found to be comparable in these materials to within the experimental error of the NMR measurement. This is a surprising result because most reports indicate that W_ϕ is nearly an order of magnitude weaker than W_θ [16]. We attribute our result to the surface roughness of the inner cavity walls. The value of the elastic constant K_{24} can also be estimated based on this transition which is completely described by the stability diagram in Fig. 3. Using the previously measured values for $W_\theta/K = (1.3 \pm 0.4) \times 10^7$ m^{-1} (from PB) and $\sigma \cong 12$ (from ET), the saddle-splay surface elastic constant is estimated to be $K_{24}/K = 1.2 \pm 1.0$ for a critical radius of $R_c = 0.5$ μm. The error is largely a reflection of the distribution of cylinder sizes and the one-constant approximation. The value of K_{24} determined above is in agreement with earlier experiment [9]. The values of K_{24}/K and W_ϕ/K could be simultaneously measured by comparing the fitting parameter σ for cavities with two different radii, if another Nuclepore sample were available with a radius of 0.6 μm. Not having this forced us to estimate the value of K_{24} by use of the stability diagram (see Fig. 3). It is worthwhile to mention that for a particularly selected system the variation of the temperature and/or radius could change the ratios RW_θ/K, RW_ϕ/K, and K_{24}/K to such extent that a reentrance of the PB structure can occur (see Fig. 3).

We have demonstrated the ability to measure both the azimuthal and polar anchoring strengths in confined cylindrical geometries using ^{2}H-NMR along with predictions from the Frank free elastic theory. The experimentally observed structural transition from the ET configuration to the newly discovered PB configuration further enables us to estimate the value of the saddle-splay surface elastic constant K_{24}. These are the first studies of this kind that allow all of these important surface parameters to be determined simultaneously by a relatively simple experiment. It is a subject of future study to reduce the error in the measurement of W_θ, W_ϕ, and K_{24} by refining the theoretical analysis: inclusion of the magnetic field term, relaxing the one-constant approximation, and including point defects due to oppositely escaping domains along the symmetry axis of the cylinder in the ET configuration.

This research was funded in part by NSF under Solid State Chemistry Grant No. 90-440635. Deuterated materials were provided by the Resource Facility of the ALCOM Science and Technology Center under DMR-89-20147.

[a]Permanent address: Department of Physics, University of Ljubljana, Jadranska 19, 61000 Ljubljana, Slovenia.

[1] B. Jerome, Rep. Prog. Phys. **54**, 391 (1991), and references therein.

[2] L. M. Blinov, A. Yu. Kabayenkov, and A. A. Sonin, Liq. Cryst. **5**, 645 (1989), and references therein.

[3] S. Faetti, M. Gatti, V. Palleschi, and T. Sluckin, Phys. Rev. Lett. **55**, 1681 (1985); K. H. Yang and C. Rosenblatt, Appl. Phys. Lett. **43**, 62 (1983); G. Barbero, E. Miraldi, C. Oldano, M. L. Rastello, and P. Valabrega, J. Phys. (Paris) **47**, 1411 (1986); H. Yokoyama, S. Kobayashi, and H. Kamei, J. Appl. Phys. **61**, 4501 (1987).

[4] D. W. Berreman, Phys. Rev. Lett. **28**, 1683 (1972); Mol. Cryst. Liq. Cryst. **23**, 215 (1973); U. Wolff, W. Greubel, and H. Kruger, Mol. Cryst. Liq. Cryst. **23**, 187 (1973); T. Oh-Ide, S. Kuniyasu, and S. Kobayashi, Mol. Cryst. Liq. Cryst. **164**, 91 (1988).

[5] F. J. Kahn, Appl. Phys. Lett. **22**, 386 (1972); J. C. Dubois, M. Gazard, and A. Zahn, J. Appl. Phys. **47**, 1270 (1976); J. Cognard, Mol. Cryst. Liq. Cryst. Suppl. **1**, 1 (1982).

[6] D. S. Seo, Y. Limura, and S. Kobayashi, Appl. Phys. Lett. **61**, 234 (1992).

[7] J. H. Erdmann, S. Zumer, and J. W. Doane, Phys. Rev. Lett. **64**, 1907 (1990).

[8] D. W. Allender, G. P. Crawford, and J. W. Doane, Phys. Rev. Lett. **67**, 1442 (1991).

[9] G. P. Crawford, D. W. Allender, and J. W. Doane, Phys. Rev. A **45**, 8693 (1992); G. P. Crawford, D. W. Allender, M. Vilfan, I. Vilfan, and J. W. Doane, Phys. Rev. A **44**, 2570 (1991).

[10] P. E. Cladis and M. Kleman, J. Phys. (Paris) **33**, 591 (1972).

[11] D. Melzer and F. R. N. Nabarro, Philos. Mag. **35**, 901 (1977).

[12] G. P. Crawford, L. M. Steele, R. Ondris-Crawford, G. S. Iannachione, C. J. Yeager, J. W. Doane, and D. Finotello, J. Chem. Phys. **96**, 7788 (1992), and references therein.

[13] T. Chen, M. J. Dipirro, B. Bhattacharyya, and F. M. Gasparini, Rev. Sci. Instrum. **51**, 846 (1980).

[14] M. Kleman, *Points, Lines, Walls in Liquid Crystals, Magnetic Systems, and Ordered Media* (Wiley, New York, 1988), and references therein.

[15] G. P. Crawford, M. Vilfan, I. Vilfan, and J. W. Doane, Phys. Rev. A **43**, 835 (1991).

[16] T. Oh-Ide, S. Kuniyasu, and S. Kobayashi, Mol. Cryst. Liq. Cryst. **164**, 91 (1988).

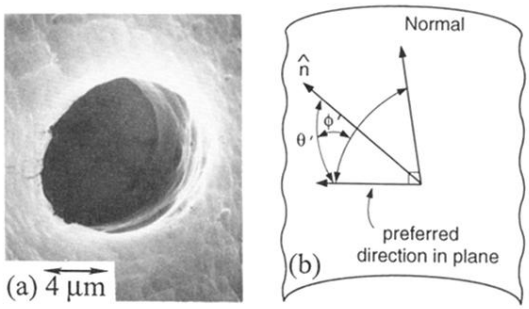

FIG. 2. The inner corrugated walls of a cylindrical cavity of Nuclepore membranes as revealed by scanning electron microscopy (SEM) (a). A representation of the angles used in the calculation of the director fields on the surface of the cavities (b).